Published OnlineFirst April 21, 2009; DOI: 10.1158/0008-5472.CAN-08-3472

Research Article

eIF4E Activation Is Commonly Elevated in Advanced Human Prostate Cancers and Significantly Related to Reduced Patient Survival

Jeremy R. Graff,[1] Bruce W. Konicek,[1] Rebecca L. Lynch,[1] Chad A. Dumstorf,[1] Michele S. Dowless,[1] Ann M. McNulty,[1] Stephen H. Parsons,[1] Leslie H. Brail,[1] Bruce M. Colligan,[2] Jonathan W. Koop,[2] Bernadette M. Hurst,[2] James A. Deddens,[3] Blake L. Neubauer,[1] Louis F. Stancato,[1] Harry W. Carter,[2] Larry E. Douglass,[2] and Julia H. Carter[2]

[1]Lilly Research Labs, Eli Lilly and Company, Indianapolis, Indiana; [2]Wood Hudson Cancer Research Laboratory, Newport, Kentucky; and [3]Department of Mathematical Sciences, University of Cincinnati, Cincinnati, Ohio

Abstract

Elevated eukaryotic translation initiation factor 4E (eIF4E) function induces malignancy in experimental models by selectively enhancing translation of key malignancy-related mRNAs (c-myc and BCL-2). eIF4E activation may reflect increased eIF4E expression or phosphorylation of its inhibitory binding proteins (4E-BP). By immunohistochemical analyses of 148 tissues from 89 prostate cancer patients, we now show that both eIF4E expression and 4E-BP1 phosphorylation (p4E-BP1) are increased significantly, particularly in advanced prostate cancer versus benign prostatic hyperplasia tissues. Further, increased eIF4E and p4E-BP1 levels are significantly related to reduced patient survival, whereas uniform 4E-BP1 expression is significantly related to better patient survival. Both immunohistochemistry and Western blotting reveal that elevated eIF4E and p4E-BP1 are evident in the same prostate cancer tissues. In two distinct prostate cancer cell models, the progression to androgen independence also involves increased eIF4E activation. In these prostate cancer cells, reducing eIF4E expression with an eIF4E-specific antisense oligonucleotide currently in phase I clinical trials robustly induces apoptosis, regardless of cell cycle phase, and reduces expression of the eIF4E-regulated proteins BCL-2 and c-myc. Collectively, these data implicate eIF4E activation in prostate cancer and suggest that targeting eIF4E may be attractive for prostate cancer therapy. [Cancer Res 2009; 69(9):3866–73]

Introduction

Eukaryotic translation initiation factor 4E (eIF4E) binds the 5′-terminal, 7-methylguanosine cap of cellular mRNAs, bringing these mRNAs to the eIF4F translation initiation complex, which then scans 5′-3′ from the cap, unwinding RNA secondary structure to reveal the translation initiation codon and enable mRNA translation. Although required for translation of all cap-dependent mRNAs, elevated eIF4E function selectively and preferentially enhances the translation of mRNAs with lengthy, highly structured 5′ untranslated regions, as these mRNAs require increased eIF4F complex activity for ribosome loading (1–3). eIF4E also promotes the nucleocytoplasmic transport of select mRNAs (4). eIF4E-regulated mRNAs generally encode proteins involved in cellular growth and survival (e.g., c-myc, BCL-2, vascular endothelial growth factor, cyclin D1, and survivin; refs. 1–4). By selectively up-regulating translation of these malignancy-related mRNAs, eIF4E overexpression in experimental models drives malignancy (5–8). Conversely, reducing eIF4E expression reverses malignancy in experimental cancer models by selectively diminishing expression of these malignancy-related mRNAs (9–12), inducing apoptosis and suppressing tumor growth, invasion, and metastasis (13–15).

eIF4E availability is regulated by the inhibitory binding proteins, the 4E-BPs. 4E-BPs bind the same residues on eIF4E necessary for the eIF4E-eIF4G interaction, thereby blocking eIF4F complex assembly and cap-dependent translation (16, 17). AKT-mammalian target of rapamycin pathway signaling elicits 4E-BP phosphorylation, which liberates eIF4E from 4E-BP, promoting eIF4F complex assembly (3, 17) and cap-dependent translation (1–3, 18, 19).

Human prostate cancers initially depend on androgens for growth and survival and, accordingly, are treated with androgen deprivation therapy. However, even with androgen deprivation, prostate cancer cells re-emerge often due to the activation of cell survival signals (20), including increased BCL-2 expression (21) and AKT pathway activation (22), both of which have been repeatedly linked to prostate cancer progression in both human prostate cancer tissues and animal prostate cancer models (21–23).

Although eIF4E activation has been associated with malignant progression in many human cancers (e.g., head and neck, bladder, colon, breast, lung, and lymphoma; ref. 1), a role for eIF4E in human prostate cancer has not been established. eIF4E may be activated by eIF4E overexpression, reduced 4E-BP expression, or 4E-BP phosphorylation elicited by AKT pathway signaling. Herein, we show that eIF4E activation is elevated significantly with progression in human and experimental prostate cancer and is significantly related to reduced patient survival. Moreover, blocking eIF4E expression in prostate cancer cells with an eIF4E-specific antisense oligonucleotide (4EASO) now in clinical trials suppresses expression of eIF4E and the eIF4E-regulated proteins, c-myc and BCL-2, robustly inducing apoptosis regardless of cell cycle phase. Collectively, these data implicate enhanced eIF4E activation in human prostate cancer progression and indicate that eIF4E may be an attractive target for prostate cancer therapy.

Materials and Methods

Cell culture, transfection, and lysate preparation. Prostate cancer cells, LNCaP (androgen-dependent) and CWR22Rv1 (androgen-independent), were purchased from the American Type Culture Collection. Androgen-independent LNAI cells were derived from LNCaP xenografts

Note: Supplementary data for this article are available at Cancer Research Online (http://cancerres.aacrjournals.org/).

Requests for reprints: Jeremy R. Graff, Lilly Research Labs, Eli Lilly and Company, DC 0546, Indianapolis, IN 46285. Phone: 317-277-0220; Fax: 317-277-3652; E-mail: Graff_jeremy@lilly.com.

doi:10.1158/0008-5472.CAN-08-3472

Published OnlineFirst April 21, 2009; DOI: 10.1158/0008-5472.CAN-08-3472

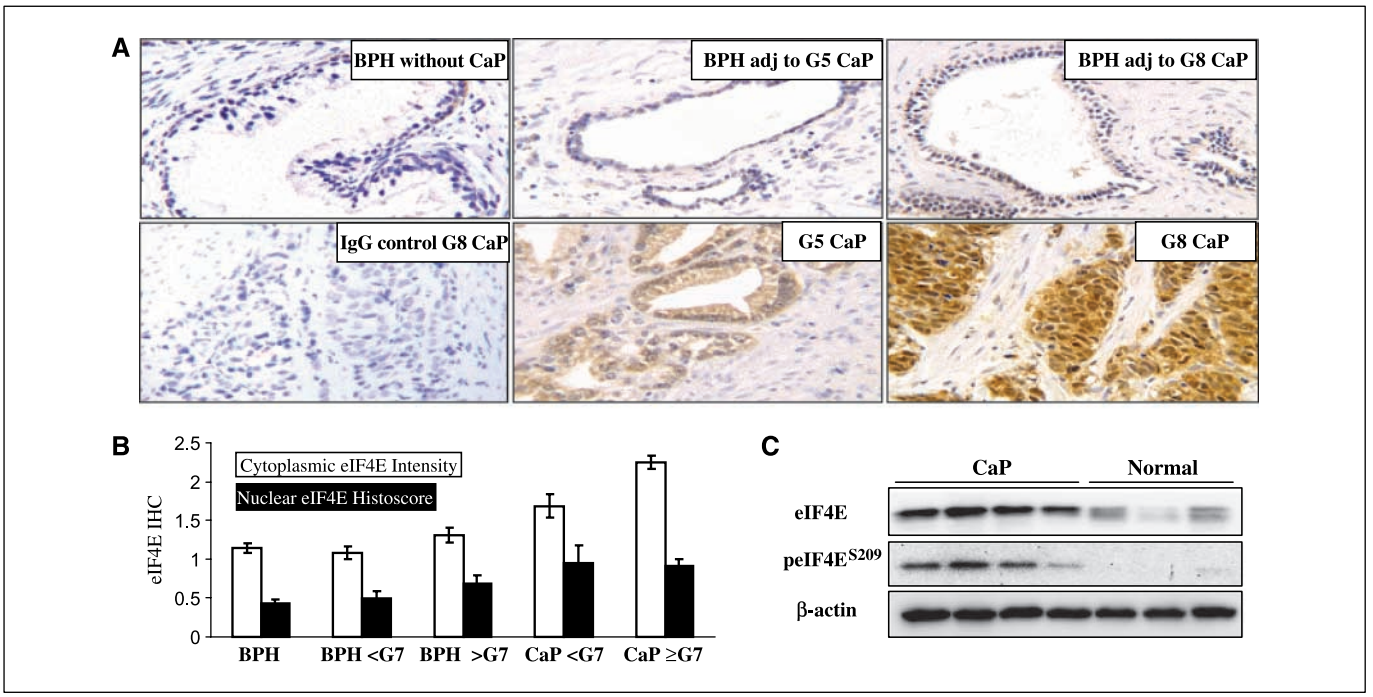

Figure 1. eIF4E expression in primary human prostate cancer tissues. *A,* representative examples of eIF4E immunohistochemistry in BPH tissue from patients without prostate cancer (*CaP*), prostate cancer tissue, and adjacent (*adj*) BPH tissue from patients with Gleason score (*G*) 5 or 8. An IgG staining control is shown. *B,* eIF4E immunohistochemistry (*IHC*) scores are shown for the five tissue groups: BPH without prostate cancer, BPH adjacent to prostate cancer with a Gleason score <7 or ≥7 or prostate cancer <7 or ≥7. *C,* Western blot analyses for eIF4E, peIF4E^{Ser209}, and β-actin in fresh-frozen human prostate cancer tissues. Each lane represents an individual patient sample.

selected for tumor growth after castration (22). Cells were transfected with 4EASO (5′-TGTCATATTCCTGGATCCTT-3′) as described (15). Lysates from cultured cells, mouse xenografts, or frozen human prostate cancer tissues were prepared for Western blotting and 7-methyl-GTP cocapture as described (15, 24). eIF4E and 4E-BP1 cocapture were executed from cell extracts by 7-methyl-GTP-Sepharose chromatography as described (25). For TaqMan quantitative reverse transcription-PCR, cDNA was generated using SuperScript III First Strand (Invitrogen) following RNA isolation with the RNeasy kit (Qiagen) and treated with DNase I (Ambion). TaqMan was done according to the manufacturer's specifications on a 7900HT Real-time PCR System (Applied Biosystems) with these primer sets (Applied Biosystems): BCL-2 (Hs00608023_m1), myc (Hs00153408_m1), β-actin (4310881E), and eIF4E (forward 5′-TGGCGACTGTCGAACCG-3′, reverse 5′-AGATTCCGTTTTCTCCTCT-3′, and probe 5′-AAACCACCCCTACTCCTAA-3′; ref. 15).

Tissues, histopathology, and clinical information. Immunohistochemistry was done on 148 archived primary prostate tissue specimens removed at surgery from 89 patients between 1986 and 1988 at St. Elizabeth Medical Center (Covington/Edgewood, KY) with institutional review board approval. For pathologic diagnosis, Gleason grade of each archived specimen was assessed by a board-certified pathologist (L.E.D.; ref. 26). Tissue consultation reports from the Department of Laboratory Medicine of St. Elizabeth Medical Center were used to confirm patient Gleason score. Clinical follow-up was obtained from the Tri-State Tumor Registry and Cancer Registry at the Hatton Cancer Care Center of St. Elizabeth Medical Center. Frozen prostate tissues were obtained from the Indiana University tumor tissue bank with institutional review board approval.

Western blot and immunohistochemical analyses. Western blots were done as described (15, 22, 24). Antibodies for immunohistochemistry and Western blotting were eIF4E (BD Biosciences; 1:150 immunohistochemistry and 1:500-1,000 Western blotting), p4E-BP1^{Ser65} (Cell Signaling Technologies; 1:100 immunohistochemistry and 1:250 Western blotting), total 4E-BP1 (Zymed/Invitrogen; 1:100 immunohistochemistry and 1:500 Western blotting), c-myc (Santa Cruz Biotechnology; 1:250 Western blotting), BCL-2 (Santa Cruz Biotechnology; 1:200 Western blotting), and β-actin (Sigma-Aldrich; 1:2,000 Western blotting). Anti-mouse and anti-rabbit IgG (Santa Cruz Biotechnology) and anti-sheep IgG (UBI) secondary antibodies were used (1:1,000).

For immunohistochemistry, antibody staining was done on 5 μm histologic sections of formalin-fixed, paraffin-embedded surgical specimens as described (27) using the DAKO AutoStainer. Each specimen had a serial section stained with nonspecific mouse IgG2b or rabbit IgG (DAKO) at a protein concentration equivalent to that used for each primary antibody tested. Each staining run included positive and negative staining controls. The LSAB2 kit (DAKO) was used for antigen detection. Sections were counterstained with hematoxylin or methyl green and coverslipped with Permount (Fisher Scientific).

Epithelial cytoplasmic and nuclear stain was evaluated semiquantitatively by two investigators (L.E.D. and J.H.C.). Stain intensity was scored on a scale of 0 to 3 (0, negative; 0.5, trace; 1, light; 2, moderate; and 3, intense). The percentage of epithelium stained was also given a numerical score (0, negative areas; 0.1, 1-25% stained; 0.4, 26-50% stained; 0.6, 51-75%; and 0.9, 76-100%). The average stain intensity and average percent area stained were determined for multiple slides and multiple fields for each specimen (between 3 and 20 fields per specimen). Histoscores were generated by multiplying average stain intensity for each tissue by average percent area stained (histoscore = intensity × area). Accordingly, the most intense, uniformly stained specimen would have a histoscore of 2.7 (3 × 0.9; ref. 27).

High-content imaging for apoptosis, cell cycle, and eIF4E expression. Cell cycle, apoptosis, and eIF4E protein expression were measured simultaneously by multiplexing activated caspase-3, TUNEL, and eIF4E immunostaining with cell-level nuclear parameters including DNA content, nuclear area, average DNA content, and DNA variation as described (28). Cells were fixed with 3.7% formaldehyde solution (Sigma-Aldrich), washed in Dulbecco's PBS (D-PBS), permeabilized with 0.1% Triton X-100/D-PBS, washed with D-PBS, and blocked 1 h in D-PBS/1% bovine serum albumin (Invitrogen). Cells were then incubated for 1 h with anti-activated caspase-3 (BD Biosciences; 1:250) and anti-eIF4E antibody (BD Biosciences; 1:150) in

Published OnlineFirst April 21, 2009; DOI: 10.1158/0008-5472.CAN-08-3472

D-PBS/1% bovine serum albumin. Cells were washed twice with D-PBS and incubated 1 h with Alexa Fluor 488 goat anti-rabbit IgG (Invitrogen; 1:250), Alexa Fluor 647 goat anti-mouse IgG (Invitrogen; 1:250), and 200 ng/mL Hoechst 33342 (Invitrogen) diluted in D-PBS/1% bovine serum albumin. Cells were washed twice in D-PBS, and TUNEL staining was done (*In situ* Cell Death Detection kit, TMR Red; Roche Biochemicals) as per the manufacturer. Stained plates were scanned using ArrayScan Vti (Cellomics) and the Target Activation Bioapplication was used for four-channel quantification of signal as described (28).

Statistical analyses. All statistical analyses were done with the SAS program (SAS). Tissues were divided into five groups: (*a*) benign prostatic hyperplasia (BPH) from patients without prostate cancer, (*b*) BPH adjacent to moderately differentiated and well-differentiated prostate cancer (Gleason score <7), (*c*) BPH adjacent to poorly differentiated, high-grade prostate cancer (Gleason score ≥7), (*d*) low-grade prostate cancer (Gleason score <7), and (*e*) high-grade prostate cancer (Gleason score ≥7). Repeated-measures ANOVAs were done to evaluate relationships between staining patterns and tissue groups 1 to 5. Tukey's adjustment method was used to obtain *P* values when comparing tissue groups. Trend analyses were used to compare staining patterns across all tissue groups. Kaplan-Meier analyses (log-rank tests) and Cox proportional hazards regression were run to assess whether the staining patterns were related to patient survival.

Results

eIF4E expression in human prostate tissues. Increased eIF4E expression has been shown in a variety of human cancers (e.g., head and neck and breast; ref. 1). However, eIF4E expression in human prostate cancer tissues has not been established. We therefore evaluated eIF4E protein expression by immunohistochemistry in 148 human primary prostate tissues from 89 prostate cancer patients. We scored eIF4E immunostaining for percent area stained and immunostaining intensity. All prostate tissues, benign or malignant, showed similar percent area stained for cytoplasmic eIF4E but varied in staining intensity (Fig. 1*A*). In BPH tissues, eIF4E cytoplasmic staining intensity is low (mean intensity score, 1.1-1.3). In low-grade prostate cancer tissues (Gleason score <7), the cytoplasmic stain intensity is increased (mean intensity score, 1.7) and further elevated in high-grade prostate cancer (Gleason score ≥7; mean intensity score, 2.3; Fig. 1*A and B*). eIF4E cytoplasmic stain intensity is significantly increased across all tissue types ($P < 0.0001$, Pearson's and Spearman's correlation coefficients), low-grade prostate cancer versus adjacent BPH ($P < 0.0001$), high-grade prostate cancer versus adjacent BPH ($P < 0.0001$), and high-grade versus low-grade prostate cancer ($P = 0.0016$; Supplementary Table S1).

Nuclear eIF4E localization has been reported previously and may mediate the nucleocytoplasmic transport of select mRNAs (e.g., cyclin D1; ref. 4). Unlike cytoplasmic staining, nuclear eIF4E staining varied in intensity and percent area stained and is therefore presented by histoscore (percent area stained × intensity; Fig. 1*A and B*). The highest nuclear eIF4E histoscores were evident in prostate cancer tissues relative to BPH tissues (Fig. 1*B*). Indeed, nuclear eIF4E histoscores were significantly increased across all tissue groups ($P = 0.0004$ and 0.0002, Pearson's and Spearman's correlation coefficients, respectively). Individual group comparisons showed significantly increased staining only in high-grade prostate cancer versus BPH from patients without prostate cancer ($P = 0.0473$; Supplementary Table S1).

These data show that eIF4E expression is elevated in prostate cancer tissues, particularly high-grade prostate cancer (Fig. 1). To

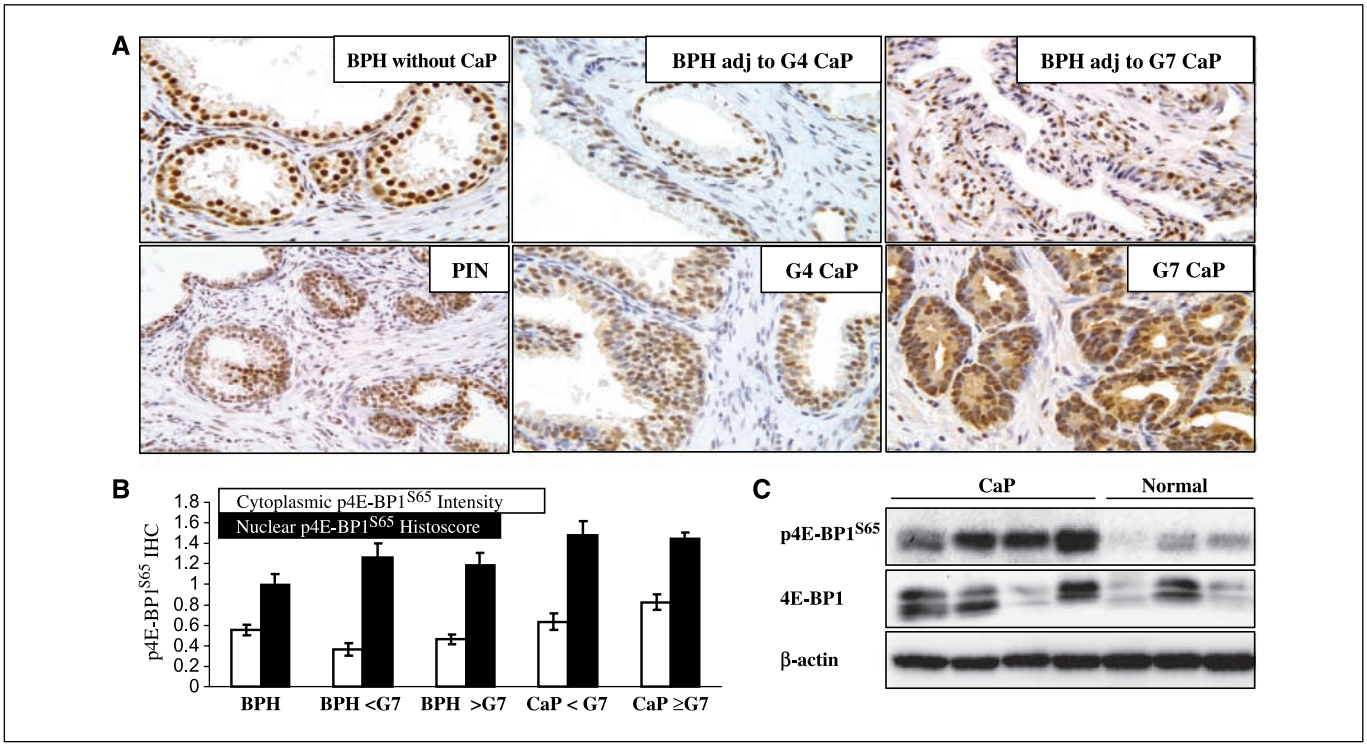

Figure 2. 4E-BP1 and p4E-BP1 expression in primary human prostate cancer tissues. *A,* representative examples of p4E-BP1^{Ser65} immunohistochemistry in BPH tissue from patients without prostate cancer (CaP), prostatic intraepithelial neoplasia (*PIN*), prostate cancer tissue, and adjacent BPH tissue from patients with Gleason score 4 or 7. *B,* p4E-BP1^{Ser65} immunohistochemistry scores are shown for five tissue groups: BPH without prostate cancer and BPH adjacent to prostate cancer with a Gleason score <7 or ≥ 7 or prostate cancer <7 or ≥7. *C,* Western blot analyses for p4E-BP1^{Ser65}, 4E-BP1 total protein, and β-actin in fresh-frozen human prostate cancer tissues. Each lane represents an individual patient sample as in Fig. 1.

Published OnlineFirst April 21, 2009; DOI: 10.1158/0008-5472.CAN-08-3472

support these immunohistochemical data, we evaluated eIF4E expression in fresh-frozen human prostate cancer tissues by Western blotting. eIF4E protein levels were markedly increased in the prostate cancer relative to benign prostate tissue samples (Fig. 1*C*) as were levels of eIF4E phosphorylation at Ser^{209} (Fig. 1*C*), a site phosphorylated by MNK kinase only when eIF4E is bound to eIF4G (with eIF4F complex assembly; refs. 1–3). These data collectively show that eIF4E expression is significantly elevated in human prostate cancer tissues.

4E-BP and p4E-BP1^{Ser65} levels in human prostate cancer samples. eIF4E may also be activated by liberation from its inhibitory binding proteins, the 4E-BPs, via 4E-BP phosphorylation at Thr^{37}, Thr^{46}, Thr^{70}, and, finally, Ser^{65} (16, 17). 4E-BP phosphorylation results from AKT-mammalian target of rapamycin pathway signaling, which is activated particularly in high-grade prostate cancer (23). We therefore examined these primary human prostate cancer tissues for 4E-BP expression and Ser^{65} phosphorylation (p4E-BP1^{Ser65}), the final residue phosphorylated before release from eIF4E (17).

4E-BP1 and p4E-BP1^{Ser65} were evident in both the cytoplasm and the nucleus of prostate tissues (Fig. 2*A*). Group-by-group comparisons revealed that total cytoplasmic and nuclear 4E-BP1 expression was similar in all groups, although by trend analyses there was a significant increase in expression across all tissue types (Supplementary Table S1). p4E-BP1^{Ser65} cytoplasmic intensity was significantly increased in prostate cancer tissues across tissue types, with the highest stain in high-grade prostate cancer (trend analyses, groups 1-5, $P < 0.0001$ and $P = 0.0018$, Pearson's and Spearman's correlation coefficients, respectively; Fig. 2*A* and *B*). Cytoplasmic p4E-BP1^{Ser65} intensity was significantly increased in high-grade prostate cancer versus adjacent BPH ($P < 0.0001$), low-grade prostate cancer versus adjacent BPH ($P = 0.0223$), and high-grade prostate cancer versus BPH from patients without prostate cancer ($P = 0.0357$; Supplementary Table S1).

Breast and ovarian cancers show nuclear p4E-BP1 stain (29, 30). Our analyses also show nuclear p4E-BP1^{Ser65} (Fig. 2). Because this stain varied in percent area stained and intensity, the data are represented as histoscores (percent area stained × intensity). Trend analyses revealed that nuclear p4E-BP1^{Ser65} histoscores were significantly increased across all tissue types ($P = 0.0028$ and 0.005, Pearson's and Spearman's correlation coefficients, respectively), with the highest nuclear histoscores evident in prostate cancer tissues (Fig. 2*B*; Supplementary Table S1). Group-by-group comparisons revealed increased nuclear p4E-BP1^{Ser65} only in high-grade prostate cancer versus BPH from patients without prostate cancer ($P = 0.0475$; Supplementary Table S1). These immunohistochemical analyses indicated that p4E-BP1^{Ser65} levels are increased in human prostate cancer versus BPH tissues. Western blotting of fresh-frozen prostate tissues also showed increased p4E-BP1^{Ser65} levels in prostate cancer, whereas total 4E-BP1 protein expression was similar, although variable, in both prostate cancer and BPH samples (Fig. 2*C*). Collectively, these data show elevated p4E-BP1^{Ser65} levels in prostate cancer tissues (Fig. 2).

Elevated eIF4E and p4E-BP1^{Ser65} levels and reduced patient survival. We next determined whether increased eIF4E and p4E-BP1^{Ser65} levels might be related to patient survival. Patients who died with prostate cancer but from other causes were excluded from these analyses. Patients were segregated into high and low eIF4E expression groups (cytoplasmic intensity score ≥2 or <2, respectively). High eIF4E expression was significantly related to

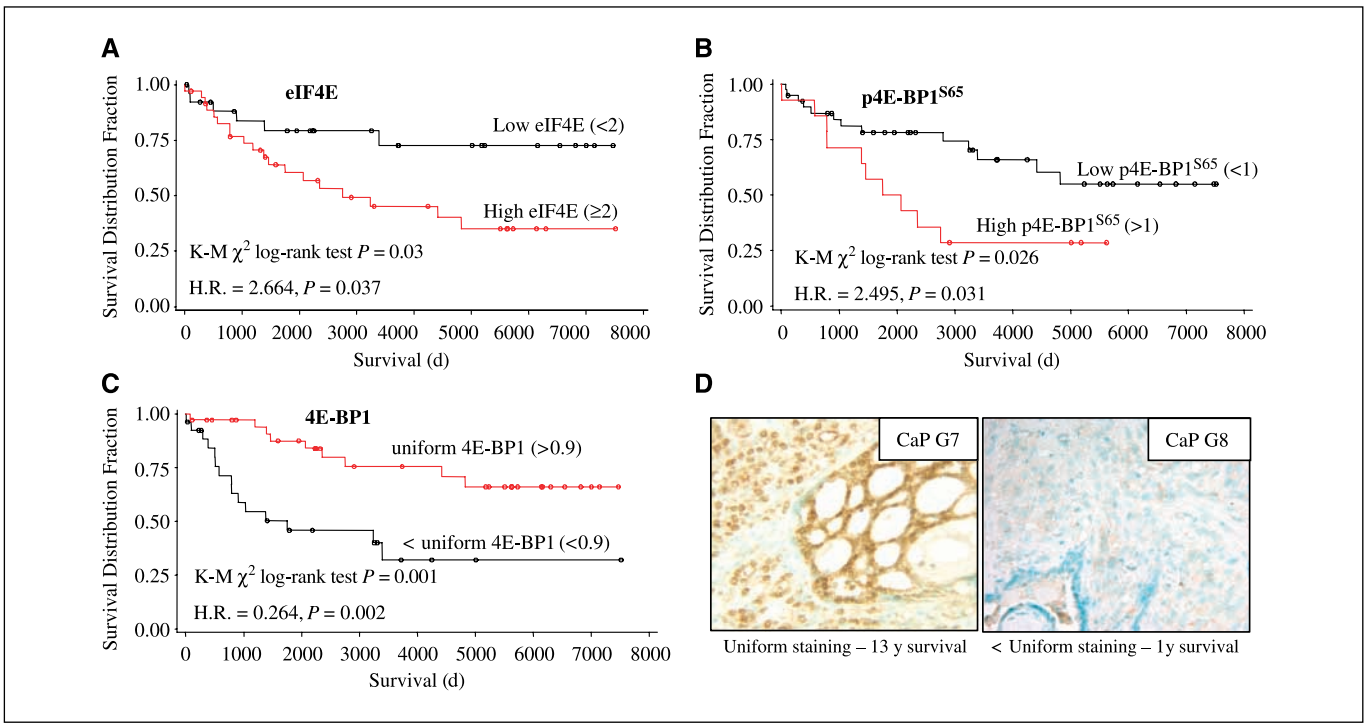

Figure 3. Kaplan-Meier survival plots for eIF4E, 4E-BP1, and p4E-BP1^{Ser65} immunostaining. *A,* prostate cancer patients were grouped based on cytoplasmic eIF4E immunohistochemical intensity. *B,* prostate cancer patients were grouped based on cytoplasmic p4E-BP1^{Ser65} immunohistochemical intensity. *C,* prostate cancer patients were grouped based on cytoplasmic 4E-BP1 expression. *A* to *C, inset,* Kaplan-Meier (*K-M*) χ^2 log-rank test values, hazard ratios (*H.R.*), and statistical significance. *D,* two prostate cancer tissues stained for 4E-BP1, both from high-grade prostate cancer (Gleason scores), one with uniform stain and one with less than uniform staining. Uniform staining indicates 76% to 100% of cells with stain (0.9).

Published OnlineFirst April 21, 2009; DOI: 10.1158/0008-5472.CAN-08-3472

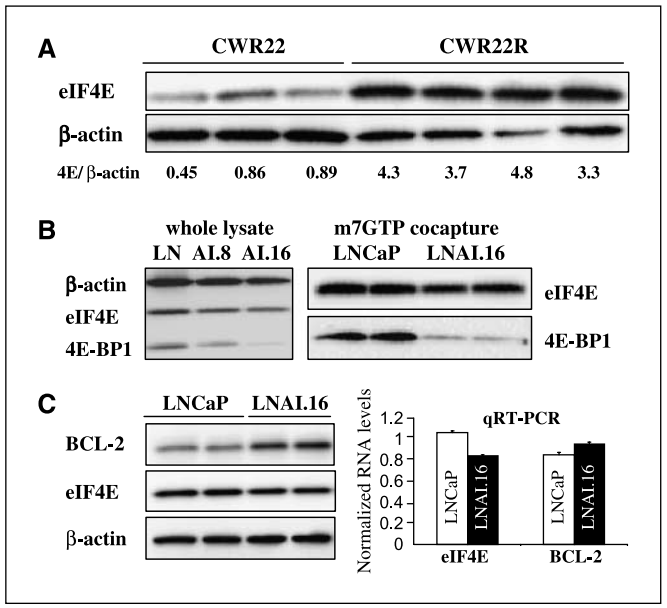

Figure 4. eIF4E activation in human prostate cancer models. *A,* Western blot analysis of eIF4E expression in tumor tissues from three androgen-dependent CWR22 and four androgen-independent CWR22R xenografts. eIF4E expression values normalized to β-actin. *B,* eIF4E, 4E-BP1, and β-actin were simultaneously assessed by Western blotting in the androgen-dependent/sensitive LNCaP (*LN*) or androgen-independent LNAI.8 (*AI.8*) and LNAI.16 (*AI.16*) cells. Blots were reprobed for β-actin to control for equal protein loading and transfer (*left*). 7-Methyl-GTP (*m7GTP*) cocapture assays were followed by Western blotting to determine eIF4E-4E-BP1 binding. Each lane represents protein harvested from a different cell culture dish (*right*). *C,* Western blots for BCL-2, eIF4E, and β-actin from duplicate LNCaP and LNAI.16 lysates. TaqMan quantitative reverse transcription-PCR (*qRT-PCR*) analyses for eIF4E and BCL-2 normalized to β-actin RNA levels ± SE from LNCaP and LNAI.16.

death from prostate cancer (Kaplan-Meier analyses χ^2 log-rank test, $P = 0.03$; Fig. 3*A*). Patients in the high eIF4E expression group were ~2.7 times likelier to die of prostate cancer than patients with low eIF4E levels (hazard ratio, 2.664; $P = 0.037$; Fig. 3*A*). Similarly, elevated p4E-BP1^{Ser65} levels (cytoplasmic intensity score >1) were also related to death from prostate cancer (Kaplan-Meier analyses χ^2 log-rank test, $P = 0.026$). Patients with high cytoplasmic p4E-BP1^{Ser65} levels were ~2.5 times likelier to die of prostate cancer (hazard ratio, 2.495; $P = 0.031$; Fig. 3*B*).

Our immunohistochemical analyses revealed that total 4E-BP1 levels were similar between individual groups. However, a fraction of patients showed reduced 4E-BP1 expression (Fig. 3*C* and *D*). These patients showed substantially reduced survival when compared with prostate cancer patients showing uniform 4E-BP1 expression (Kaplan-Meier analyses, log-rank test, $P = 0.001$). Patients whose prostate cancer tissues showed uniform 4E-BP1 expression were only ~25% as likely to die of prostate cancer as patients whose tumors showed reduced 4E-BP1 immunostaining (hazard ratio, 0.264; $P = 0.002$; Fig. 3*C* and *D*).

Elevated eIF4E in experimental prostate cancer. The immunohistochemical analyses revealed that eIF4E and p4E-BP1 levels are elevated and related to reduced prostate cancer patient survival. We therefore evaluated whether eIF4E activation may also be enhanced in experimental models of prostate cancer progression to androgen independence, the CWR22-CWR22R (31) and LNCaP-LNAI (22) models. Western blotting showed that eIF4E expression was substantially elevated in four separate hormone-refractory CWR22R xenograft samples versus three separate CWR22 hormone-dependent xenografts (Fig. 4*A*). To account for the variable tissue content of xenograft tumors (murine endothelial and stromal tissues plus healthy and necrotic human prostate cancer tissues), multiple tumors are depicted for each line and the expression of eIF4E normalized to β-actin is shown for each xenograft. CWR22 prostate cancer tumors are PTEN-positive. There were no substantial differences between CWR22 and CWR22R in levels of total or phosphorylated 4E-BP1 (data not shown).

In the LNCaP-LNAI model, eIF4E levels were largely unchanged, but 4E-BP1 protein expression was substantially reduced, particularly in the aggressive, androgen-independent LNAI.16 cells (Fig. 4*B*). These LNAI cells show AKT hyperactivation relative to the hormone-dependent LNCaP cells (22). Accordingly, LNAI.16 show >2-fold increase in p4E-BP1^{Ser65} levels versus LNCaP (data not shown). We therefore assessed the amount of eIF4E bound to 4E-BP1 using the 7-methyl-GTP (mRNA cap-analogue) bead cocapture assay (25). Consistent with reduced 4E-BP1 expression and increased 4E-BP1 phosphorylation, LNAI.16 cells show decreased levels of 4E-BP1 bound to eIF4E versus LNCaP (Fig. 4*B*), indicating increased eIF4E function in LNAI cells. Indeed, expression of the eIF4E-regulated protein BCL-2 is increased 2.4-fold in LNAI versus LNCaP, whereas BCL-2 RNA levels are virtually unchanged (Fig. 4*C*). Together, these data provide evidence that androgen-independent prostate cancer cells up-regulate eIF4E, either directly by overexpression (CWR22R) or indirectly, via increased AKT pathway signaling (22) and reduced 4E-BP1 expression (LNAI).

Reducing eIF4E in prostate cancer cells induces apoptosis regardless of cell cycle phase. Immunohistochemistry and

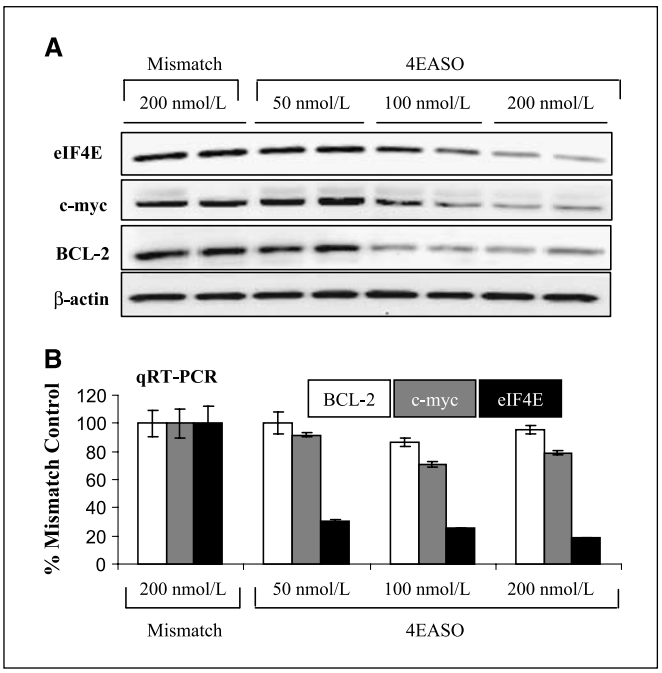

Figure 5. Reducing eIF4E expression in prostate cancer cells suppresses expression of eIF4E-regulated proteins. *A,* Western blot analyses for eIF4E, c-myc, BCL-2, and β-actin in CWR22Rv1 prostate cancer cells 72 h after transfection with the 4EASO or mismatch control ASO (50-200 nmol/L). Blots were reprobed for β-actin to control for equal protein loading and transfer. *B,* TaqMan quantitative reverse transcription-PCR analyses for BCL-2 (*white*), c-myc (*gray*), and eIF4E (*black*) normalized to β-actin RNA and relative to the mismatch ASO-transfected controls. RNA was harvested from the same transfections represented in *A*. Data represent at least three transfection experiments.

Published OnlineFirst April 21, 2009; DOI: 10.1158/0008-5472.CAN-08-3472

Western blot analyses of prostate cancer tissues and cells implicate elevated eIF4E function in prostate cancer, particularly in advanced disease. Increased eIF4E function would selectively enhance the translation of mRNAs with lengthy, G+C-rich 5′ untranslated regions (e.g., c-myc and BCL-2), enabling prostate cancer tumor growth and survival (1). Reducing eIF4E function may therefore be an effective therapeutic strategy for prostate cancer (32). Indeed, we recently showed that a 4EASO effectively reduced eIF4E expression in a wide array of cancer cells, repressing expression of eIF4E-regulated proteins (e.g., c-myc and BCL-2) and inducing apoptosis. Intravenous administration of this 4EASO effectively suppressed growth of breast and prostate cancer xenografts, reducing eIF4E protein expression, inducing apoptosis, and reducing cellular proliferation in the treated xenograft tissues (15). We sought to extend these data to additional prostate cancer cells to explore further the potential of the 4EASO for prostate cancer treatment.

Transfection with the 4EASO reduced eIF4E protein expression in CWR22Rv1 cells. Consistent with its mechanism of action, the 4EASO specifically targets eIF4E mRNA for degradation (15), subsequently decreasing eIF4E protein expression. Reduced eIF4E protein would then suppress expression of eIF4E-regulated proteins. Accordingly, 4EASO transfection resulted in reduced expression of the eIF4E-regulated proteins c-myc and BCL-2 (Fig. 5*A*), both of which have been linked to the emergence of advanced, hormone-independent disease (33, 34). 4EASO transfection did not markedly reduce c-myc or BCL-2 RNA levels (Fig. 5B). These data support the notion that blocking eIF4E function would primarily suppress expression of eIF4E-regulated proteins without substantially affecting mRNA levels for these proteins (1, 15, 32).

We next evaluated the biological consequences of reducing eIF4E expression in prostate cancer cells. In both LNCaP and CWR22Rv1, 4EASO transfection robustly induced apoptosis as evidenced by increased TUNEL staining and an overall reduction in cell number (Hoechst-stained nuclei; Fig. 6*A* and *B*). To assess whether apoptosis elicited by eIF4E reduction may be induced in one or more phases of the cell cycle, we used high-content cellular imaging (28) to evaluate simultaneously cell cycle phase, apoptosis (TUNEL and activated caspase-3 staining), and eIF4E expression. Cell cycle was determined by simultaneously monitoring nuclear DNA content, nuclear area, average DNA content, and DNA variation as described (28). For each cell line and treatment, >1,000 cells were evaluated. The data are displayed as a heat map (lowest levels in blue and highest in red) with the cell cycle phase shown to the right. Each horizontal line represents a single cell. In both LNCaP and CWR22Rv1 cells, eIF4E reduction was evident in cells treated with 4EASO versus mismatch in all phases of the cell cycle (represented by the preponderance of blue lines after 4EASO transfection). In these same 4EASO-treated cells, activated caspase-3 and TUNEL staining were increased versus mismatch ASO-transfected cells and evident in cells in all phases of the cell cycle (horizontal lines show increased yellow-to-red intensity). The greatest positivity for both markers of apoptosis is evident in cells in late S to M phase of the cell cycle (Fig. 6*A* and *B*). These data indicate that reducing eIF4E in prostate cancer cells elicits apoptosis in a cell cycle phase-independent manner.

Discussion

The emergence of hormone-refractory, castration-independent prostate cancer is driven by activation of survival pathways (e.g., increased expression of the antiapoptotic oncogene BCL-2 and AKT pathway activation; refs. 20–22). AKT pathway activation, in particular, has been repeatedly linked to prostate cancer progression in both human prostate cancer tissues and animal models of prostate cancer (22, 23). eIF4E is activated downstream of AKT and may be a critical effector molecule of the AKT pathway (8).

Data presented herein show that eIF4E activation is commonly elevated with advanced disease in both human primary prostate cancer tissues and prostate cancer cells. Both eIF4E expression and 4E-BP phosphorylation are elevated in high-grade primary human prostate cancer tissues, particularly advanced disease, and

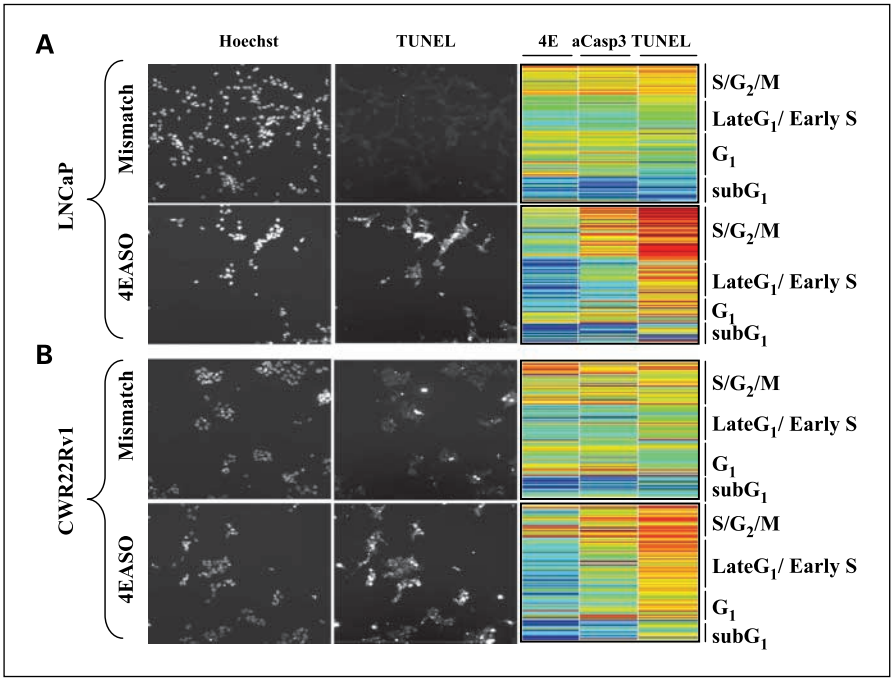

Figure 6. Reducing eIF4E expression in prostate cancer cells induces apoptosis. Representative photomicrographs for Hoechst nuclear staining and TUNEL staining for (*A*) LNCaP (48 h) or (*B*) CWR22Rv1 (72 h) prostate cancer cells transfected with the mismatch control or 4EASO (100 nmol/L). Note the punctate TUNEL staining evident in the 4EASO-treated cells. Representative heat maps for LNCaP (*A*) and CW22Rv1 (*B*) from high-content imaging of these transfections enable simultaneous evaluation of eIF4E expression as well as markers of apoptosis, activated caspase-3 (*aCasp3*), and TUNEL staining. Nuclear DNA content, nuclear area, average DNA content, and DNA variation were also measured to determine cell cycle phase as described (28). *Right,* cell cycle phase. *Horizontal line,* single cell. Data are sorted and displayed based on DNA content. Lower than average signal intensity is shown in blue, higher than average in yellow, then red. Data represent 1,021 LNCaP cells from mismatch ASO transfections and 1,250 from the 4EASO transfections (*A*). For CWR22Rv1, data represent 1,135 cells from the mismatch control ASO-treated cells and 1,058 cells treated with 100 nmol/L 4EASO (*B*). Representative of three or more separate transfection experiments for each cell line.

Published OnlineFirst April 21, 2009; DOI: 10.1158/0008-5472.CAN-08-3472

significantly related to reduced patient survival. In a minority of patients who die very quickly of disease, 4E-BP1 protein expression is significantly reduced. In two separate experimental prostate cancer models, progression to androgen independence involves increased eIF4E activation either by eIF4E overexpression or by reduced 4E-BP1 expression and binding to eIF4E. In these same models, blocking eIF4E expression with a 4EASO robustly induces apoptosis and suppresses expression of the eIF4E-regulated proteins c-myc and BCL-2, both of which have been linked to prostate cancer progression (33, 34). Taken together, these data implicate enhanced eIF4E function in malignant prostate cancer progression and suggest that targeting eIF4E may be an attractive strategy for prostate cancer therapy.

Enhanced eIF4E activation has been reported in a variety of human and experimental cancers as a result of either elevated eIF4E expression or decreased 4E-BP1 function (1, 35). Like recent reports in breast and ovarian cancers, our data in prostate cancer now also show p4E-BP1 and 4E-BP1 staining in the nucleus, with cytoplasmic p4E-BP1 staining restricted to tumor tissue (29, 30). Our data now also reveal that elevated eIF4E and p4E-BP1^{Ser65} levels are evident in the same samples, suggesting that prostate cancer progression may involve both eIF4E up-regulation and increased AKT pathway signaling.

Previous reports in gastric carcinoma (36), prostate (37), and breast (38) carcinomas have shown increased 4E-BP1 expression in advanced malignancies. In this study, there were no significant differences in 4E-BP1 expression between individual tissue groups, but there was a trend for increased expression in the highest-grade prostate cancer samples. The selection for such increased 4E-BP1 expression is unclear, although it may reflect a reliance on both cap-independent and cap-dependent protein translation as suggested recently for inflammatory breast cancers (38).

Although there was a trend for increased 4E-BP1 expression in this study, a minority of prostate cancer tissues showed markedly reduced 4E-BP1 expression and this reduction was significantly associated with dramatically shortened survival (Fig. 3*C* and *D*). Consistent with a previous report relating reduced 4E-BP1 levels with pathologic stage $\geq T_3$ (37), these data suggest that loss of 4E-BP1 may portend a particularly poor prognosis in a minority of prostate cancer patients.

Prostate cancer has a notoriously low rate of proliferation (<5% Ki-67-positive), even in high-grade, recurrent, and metastatic prostate cancer (39), indicating that prostate cancer progression is characterized by relentless prostate cancer cell survival. As such, therapies targeting survival pathways, particularly in a cell cycle-independent manner, may be particularly attractive for prostate cancer treatment (20, 39). eIF4E suppresses the apoptotic response to many proapoptotic insults including thapsigargin (40–42), which has been repeatedly proposed as a putative prostate cancer therapeutic (20). Our data now extend these observations, showing that reduction of eIF4E robustly induces apoptosis in either LNCaP or CWR22Rv1 cells and that apoptosis is evident in all phases of the cell cycle. As suggested for thapsigargin (20), the induction of apoptosis in a cell cycle phase-independent manner may be particularly important for prostate cancer therapy where the proportion of cycling cells is low.

With our earlier reports showing that 4EASO treatment induces apoptosis in, and suppresses growth of, PC-3 human prostate cancer xenografts (15), the data in this report further substantiate the notion that eIF4E might be an attractive target for prostate cancer therapy and have prompted the advance of the 4EASO into cancer clinical trials (32).

Disclosure of Potential Conflicts of Interest

J.R. Graff, B.W. Konicek, R.L. Lynch, C.A. Dumstorf, M.S. Dowless, A.M. McNulty, S.H. Parsons, L.H. Brail, B.L. Neubauer, and L.F. Stancato are all employees and shareholders of Eli Lilly and Company. J.R. Graff: patent on 4EASO. B.M. Colligan, J.W. Koop, B.M. Hurst, H.W. Carter, L.E. Douglass, and J.H. Carter are all employees of the Wood Hudson Cancer Research Laboratory, which has received grant funding from Eli Lilly and Company. J.A. Deddens declared no potential conflicts of interest.

Acknowledgments

Received 9/12/08; revised 12/23/08; accepted 2/4/09; published OnlineFirst 4/21/09.

Grant support: Eli Lilly and Company (B.M. Colligan, J.W. Koop, B.M. Hurst, H.W. Carter, L.E. Douglass, and J.H. Carter).

The costs of publication of this article were defrayed in part by the payment of page charges. This article must therefore be hereby marked *advertisement* in accordance with 18 U.S.C. Section 1734 solely to indicate this fact.

We thank Charles Cohen for reviewing this article, Drs. Gaynor, Pearce, Blanchard, and Starling for supporting this work, Dr. J. Pemberton and the staff of the Hatton Cancer Care Center at St. Elizabeth Medical Center, and Dr. S. Williams and the Indiana University School of Medicine.

This work is dedicated to the memory of Dr. H.W. Carter, a wonderful colleague, teacher, and friend.

References

1. De Benedetti A, Graff JR. eIF4E expression and its role in malignancies and metastases. Oncogene 2004;23:3189–99.
2. Mamane Y, Petroulakis E, Rong L, Yoshida K, Ler LW, Sonenberg N. eIF4E-from translation to transformation. Oncogene 2004;23:3172–9.
3. Proud CG. Signalling to translation: how signal transduction pathways control the protein synthetic machinery. Biochem J 2007;403:217–34.
4. Culjkovic B, Topisirovic I, Skrabanek L, Ruiz-Gutierrez M, Borden KL. eIF4E is a central node of an RNA regulon that governs cellular proliferation. J Cell Biol 2006;175:415–26.
5. Lazaris-Karatzas A, Montine KS, Sonenberg N. Malignant transformation by a eukaryotic initiation factor subunit that binds to mRNA cap. Nature 1990;345:544–7.
6. Zimmer SG, DeBenedetti A, Graff JR. Translational control of malignancy: the mRNA cap-binding protein, eIF4E, as a central regulator of tumor formation, growth, invasion and metastasis. Anticancer Res 2000;20:1343–51.
7. Ruggero D, Montanaro L, Ma L, et al. The translation factor eIF4E promotes tumor formation and cooperates with c-Myc in lymphomagenesis. Nat Med 2004;10:484–6.
8. Wendel HG, De Stanchina E, Fridman JS, et al. Survival signalling by Akt and eIF4E in oncogenesis and cancer therapy. Nature 2004;428:332–7.
9. Rinker-Schaeffer CW, Graff JR, DeBenedetti A, Zimmer SG, Rhoads RE. Decreasing the level of translation initiation factor 4E with antisense RNA causes reversal of ras-mediated transformation and tumorigenesis of cloned rat embryo fibroblasts. Int J Cancer 1993;55:841–7.
10. Graff JR, Boghaert ER, DeBenedetti A, Tudor DM, Zimmer SG. Reduction of translation initiation factor 4E reduces tumor growth, invasion and metastasis of ras-transformed cloned rat embryo fibroblast. Int J Cancer 1995;60:255–63.
11. Nathan CA, Carter P, Liu L, et al. Elevated expression of eIF4E and FGF-2 isoforms during vascularization of breast carcinomas. Oncogene 1997;15:1087–95.
12. DeFatta RJ, Nathan CA, DeBenedetti A. Antisense RNA to eIF4E suppresses oncogenic properties of a head and neck squamous cell carcinoma cell line. Laryngoscope 2000;110:928–33.
13. Rousseau D, Gingras AC, Pause A, Sonenberg N. The eIF4E-binding proteins 1 and 2 are negative regulators of cell growth. Oncogene 1996;13:2415–20.
14. Herbert TP, Fahraeus R, Prescott A, Lane DP, Proud CG. Rapid induction of apoptosis mediated by peptides that bind initiation factor 4E. Curr Biol 2000;10:793–6.
15. Graff JR, Konicek BW, Vincent TM, et al. Therapeutic suppression of translation initiation factor eIF4E expression reduces tumor growth without toxicity. J Clin Invest 2007;117:2638–48.
16. Brunn GJ, Hudson CC, Sekulic A, et al. Phosphorylation of the translational repressor PHAS-1 by the mammalian target of rapamycin. Science 1997;277:99–101.
17. Gingras AC, Kennedy SG, O'Leary MA, Sonenberg N, Hay N. 4E-BP1, a repressor of the mRNA translation, is phosphorylated and inactivated by the Akt (PKB) signaling pathway. Genes Dev 1998;12:502–13.
18. Larsson O, Perlman DM, Fan D, et al. Apoptosis resistance downstream of eIF4E: posttranscriptional activation of an anti-apoptotic transcript carrying a consensus hairpin structure. Nucleic Acids Res 2006;34:4375–86.
19. Mamane Y, Petroulakis E, Martineau Y, et al.

Epigenetic activation of a subset of mRNAs by eIF4E explains its effects on cell proliferation. PLoS ONE 2007; 2:e242.
20. Uzgare AR, Isaacs JT. Prostate cancer: potential targets of anti-proliferative and apoptotic signaling pathways. Int J Biochem Cell Biol 2005;37:707–14.
21. Liu AY, Corey E, Bladou F, Lange PH, Vessella RL. Prostatic cell lineage markers: emergence of $BCL2^+$ cells of human prostate cancer xenograft LuCaP 23 following castration. Int J Cancer 1996;65:85–9.
22. Graff JR, Konicek BW, McNulty AM, et al. Increased AKT activity contributes to prostate cancer progression by dramatically accelerating prostate tumor growth and diminishing $p27^{Kip1}$ expression. J Biol Chem 2000;275: 24500–5.
23. Majumder PK, Sellers WR. Akt-regulated pathways in prostate cancer. Oncogene 2005;24:7465–74.
24. Graff JR, McNulty AM, Hanna KR, et al. The protein kinase Cβ-selective inhibitor, enzastaurin (LY317615.HCl), suppresses signaling through the AKT pathway, induces apoptosis, and suppresses growth of human colon cancer and glioblastoma xenografts. Cancer Res 2005;65:7462–9.
25. Wang X, Proud CG. Methods for studying signal-dependent regulation of translation factor activity. Methods Enzymol 2007;431:136–7.
26. Gleason DF. Histologic grading of prostate cancer: a perspective. Hum Pathol 1992;23:273–9.
27. Carter JH, Douglass LE, Deddens JA, et al. Pak-1 expression increases with progression of colorectal carcinomas to metastasis. Clin Cancer Res 2004;10: 3448–56.
28. Low JA, Huang S, Dowless MS, et al. High content imaging characterization of cell cycle therapeutics through *in vitro* and *in vivo* subpopulation analysis. Mol Cancer Ther 2008;7:2455–63.
29. Rojo F, Najera L, Lirola J, et al. 4E-binding protein 1, a cell signaling hallmark in breast cancer that correlates with pathologic grade and prognosis. Clin Cancer Res 2007;13:81–9.
30. Castellvi J, Garcia A, Rojo F, et al. Phosphorylated 4E-binding protein 1: a hallmark of cell signaling that correlates with survival in ovarian cancer. Cancer 2006; 107:1801–11.
31. Gregory CW, Johnson RT, Jr., Mohler JL, French FS, Wilson EM. Androgen receptor stabilization in recurrent prostate cancer is associated with hypersensitivity to low androgen. Cancer Res 2001;61:2892–8.
32. Graff JR, Konicek BW, Carter JH, Marcusson EG. Targeting the eukaryotic translation initiation factor 4E for cancer therapy. Cancer Res 2008;68:631–4.
33. Colombel M, Symmans F, Gil S, et al. Detection of the apoptosis-suppressing oncoprotein bc1-2 in hormone-refractory human prostate cancers. Am J Pathol 1993; 143:390–400.
34. Nupponen NN, Kakkola L, Koivisto P, Visakorpi T. Genetic alterations in hormone-refractory recurrent prostate carcinomas. Am J Pathol 1998;153:141–8.
35. Avdulov S, Li S, Michalek V, et al. Activation of translation complex eIF4F is essential for the genesis and maintenance of the malignant phenotype in human mammary epithelial cells. Cancer Cell 2004;5: 553–63.
36. Martín ME, Pérez MI, Redondo C, Alvarez MI, Salinas M, Fando JL. 4E binding protein 1 expression is inversely correlated to the progression of gastrointestinal cancers. Int J Biochem Cell Biol 2000;32:633–42.
37. Kremer CL, Klein RR, Mendelson J, et al. Expression of mTOR signaling pathway markers in prostate cancer progression. Prostate 2006;66:1203–12.
38. Braunstein S, Karpisheva K, Pola C, et al. A hypoxia-controlled cap-dependent to cap-independent translation switch in breast cancer. Mol Cell 2007;28: 501–12.
39. Berges RR, Vukanovic J, Epstein JI, et al. Implication of cell kinetic changes during the progression of human prostatic cancer. Clin Cancer Res 1995;1:473–80.
40. Polunovsky VA, Rosenwald IB, Tan AT, et al. Translational control of programmed cell death: eukaryotic translation initiation factor 4E blocks apoptosis in growth-factor-restricted fibroblasts with physiologically expressed or deregulated Myc. Mol Cell Biol 1996; 16:6573–81.
41. Li S, Perlman DM, Peterson MS, et al. Translation initiation factor 4E blocks endoplasmic reticulum-mediated apoptosis. J Biol Chem 2004;279:21312–7.
42. Li S, Takasu T, Perlman DM, et al. Translation factor eIF4E rescues cells from Myc-dependent apoptosis by inhibiting cytochrome c release. J Biol Chem 2003;278: 3015–22.

Cancer Research
The Journal of Cancer Research (1916–1930) | The American Journal of Cancer (1931–1940)

AACR American Association for Cancer Research

eIF4E Activation Is Commonly Elevated in Advanced Human Prostate Cancers and Significantly Related to Reduced Patient Survival

Jeremy R. Graff, Bruce W. Konicek, Rebecca L. Lynch, et al.

Cancer Res 2009;69:3866-3873. Published OnlineFirst April 21, 2009.